Nonpeptidic Inhibitors of Human Leukocyte Elastase. 3.[1] Design, Synthesis, X-ray Crystallographic Analysis, and Structure–Activity Relationships for a Series of Orally Active 3-Amino-6-phenylpyridin-2-one Trifluoromethyl Ketones

Peter R. Bernstein,*,† Don Andisik,† Prudence K. Bradley,‡ Craig B. Bryant,† Christopher Ceccarelli,‡ James R. Damewood, Jr.,‡ Roger Earley,§ Philip D. Edwards,† Scott Feeney,† Bruce C. Gomes,⊥ Benedict J. Kosmider,† Gary B. Steelman,† Roy M. Thomas,† Edward P. Vacek,† Chris A. Veale,† Joseph C. Williams,⊥ Donald J. Wolanin,†,∥ and Sheila A. Woolson†

Zeneca Pharmaceuticals Group, A Business Unit of ZENECA Inc., 1800 Concord Pike, Wilmington, Delaware 19897

Received June 8, 1994®

A series of nonpeptidic inhibitors of human leukocyte elastase (HLE) is reported. These trifluoromethyl ketone-based inhibitors contain a 3-amino-6-phenylpyridone group as a central template. The effect of varying the N-3 substituent in these inhibitors on in vitro potency, physical properties, and oral activity in a hamster based, HLE-induced lung damage model is described. The variety of substituents at this position that have little effect on in vitro potency supports the idea that this region of the molecule does not interact strongly with the enzyme. One exception to this generality is **13k**, which is substituted with a (4-acetamidophenyl)sulfonyl group. This compound has a K_i of 0.7 nM and is, in vitro, the most potent inhibitor in the series. In contrast, variation of the N-3 substituent was found to have a dramatic effect on activity after oral administration. Several analogs, including the parent amine, **7**, formamide, **2u**, benzyl sulfamide, **13e**, and benzyl sulfonamide, **13f**, show significant activity when administered at an oral dose of 2.5 mg/kg. Support for the modeling-based design concepts was obtained through in vitro SAR results and X-ray crystallographic analysis of the complex between **13d** and porcine pancreatic elastase (PPE), a closely related enzyme.

Introduction

Human leukocyte elastase (HLE, EC 3.4.21.37)[2] is a serine proteinase that has been implicated as a causative or contributory agent in several pathological states.[3] This has resulted in a wide-ranging search for low molecular weight inhibitors of HLE that might serve as therapeutic agents. Many types of peptidic and nonpeptidic inhibitors, employing both reversible and nonreversible mechanisms of action, have been reported.[4]

Our goal is to develop orally acting, nonpeptidic, reversible inhibitors of HLE for use in disease states in which elastolytic activity is ineffectively controlled by endogenous inhibitors. We have recently described the development of a series of pyridone-containing, reversible, trifluoromethyl ketone-based, inhibitors of HLE (e.g., **1** and **2a**, Figure 1).[1] While high levels of in vitro potency were attained for these compounds (e.g., **2a**), they lacked the desired oral activity. In this paper, we describe efforts that led to both increased in vitro activity and to orally active pyridone-based inhibitors.

Pyridone **2a** was selected, as a prototypical compound, for detailed investigation of its pharmacokinetic and physical properties in order to obtain the information necessary for developing a pathway forward to orally active derivatives. Physicochemical studies showed **2a** to be both very insoluble and lipophilic (see Table 2). With such a physicochemical profile, poor bioavailability, protein binding, etc., could be significant barriers to obtaining the desired oral activity.

To ascertain whether poor oral bioavailability was a limiting factor, pharmacokinetic studies were conducted in rats, using two different formulations of the compound (see Table 1). Oral administration of **2a** in 50% PEG/PBS[5] resulted in no detectable blood levels of drug or apparent metabolites. However, when the formulation was changed to a solution of **2a** in a 45/55 mixture of (2-hydroxypropyl)-β-cyclodextrin and PBS, significant blood levels were achieved at 25 mg/kg, and the bioavailability of the compound was determined to be 59%. The formation of a solubilizing inclusion complex[6] with **2a** was hypothesized as the origin of this cyclodextrin-assisted increase in bioavailability.

The high degree of lipophilicity for **2a** also suggested that the lack of oral activity could, in part, be due to extensive protein binding in vivo. In vitro, measurement of the K_i of **2a** in the presence of 5.6% human serum albumin resulted in a factor of 14.5 decrease in potency, highlighting this concern.

The above results implied that the lack of oral activity for **2a** was likely due to poor absorption and/or affinity for plasma proteins. We therefore began the preparation of analogs of **2a** that were more soluble and less lipophilic and that, at the same time, retained high levels of in vitro potency. The foundation for these efforts was the previously reported structural recognition elements for the interaction of pyridones with HLE (see Figure 2 and discussion in ref 1c).

In designing less lipophilic, more soluble pyridone inhibitors, it was our intent to preserve these key interactions. Throughout this design process, molecular modeling played a key role in determining which regions of the inhibitor were available for modification and which modifications could be expected to result in HLE inhibitors that maintained these key interactions.

Structural analysis using the ENIGMA[7] molecular

† Department of Medicinal Chemistry.
‡ Structural Chemistry Section, Department of Medicinal Chemistry.
⊥ Department of Pharmacology.
§ Drug Disposition and Metabolism Department.
∥ Current address: Miles Pharmaceuticals, West Haven, CT.
® Abstract published in *Advance ACS Abstracts*, September 1, 1994.

0022-2623/94/1837-3313$04.50/0

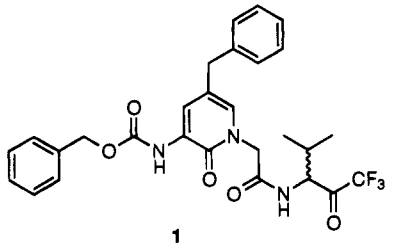

1

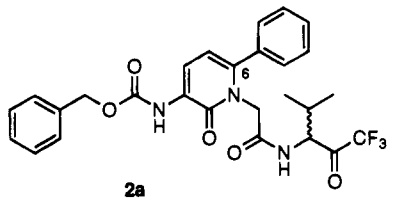

2a

Figure 1. Lead pyridone-based inhibitors.

Table 1. Pharmacokinetic Parameters for Selected Inhibitors[a]

compd	oral dose (mg/kg)	formulation	species	N^b	$C_{max}{}^d$ (ng/mL)	$T_{max}{}^e$	$t_{1/2}$ (po)^f	(%) oral bioavailability
2a	37.5	50% PEG/PBS	rat	2	not detected[c]	–	–	
2a	25.0	45% HPCD/PBS	rat	4	1886	1.4 h	3.0 h	59
2e	60.0	10% PEG/water at pH 3	hamster	3	75	3.0 h	NC	2
2o	40.0	10% PEG/water at pH 3	hamster	3	2774	0.25 h	1.3 h	45
2o	5.0	10% PEG/water at pH 3	dog	3	3151	1.0 h	0.8 h	~100
2r	40.0	10% PEG/water	hamster	3	2779	0.25 h	1.9 h	35

[a] Abbreviations are defined in ref 2. [b] N = number of animals used in study. [c] Limit of detection = 200 ng/mL, blood levels examined out to 4 h postdose. [d] Maximum concentration of unchanged drug in plasma recorded in the period 0–6 h postdose. Only three significant digits. [e] Time of maximum drug concentration. [f] Pharmacokinetic half-life.

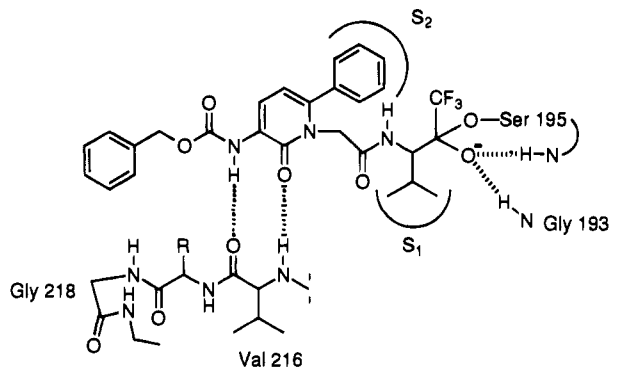

Figure 2. Proposed binding interactions between inhibitors and HLE.

graphics system and the associated AESOP[8] molecular mechanics program, suggested that all of the indicated (see Figure 2) HLE–pyridone binding interactions could be obtained for **2a**. These in vacuo molecular-mechanics minimizations also showed the benzyl portion of the CBZ group nestled onto the surface of the enzyme (near Gly-218). In contrast, aqueous molecular dynamics (MD)[9] simulations revealed that the benzyl portion of the CBZ group remained quite exposed to the aqueous environment, spending only moderate periods of time in contact with the enzyme surface. These MD simulations suggested the potential to modify the CBZ group while maintaining high levels of in vitro activity (Figure 3).

Previous SAR studies in both the parent pyridone and the 5-benzylpyridone series had shown that in vitro potency could be retained upon replacement of the CBZ group with selected hydrophilic substituents.[1b] Additionally, modification of the 3-amino substituent had synthetic advantages that would allow a number of compounds with differing physicochemical characteristics to be made quickly. This would enable us to rapidly determine those properties that were most advantageous for producing oral activity. As a result of these observations, efforts were directed toward modification of the physical properties of the pyridone inhibitors through alteration of the 3-amino substituent.[10]

Synthetic Chemistry

The compounds reported in this study were prepared (see Schemes 1–5) starting with pyridones **3** and **4**.[1c] Initially we utilized the sequences illustrated in Scheme 1. Aminopyridone **4** is a versatile intermediate that can be converted to pyridone–TFMKs (**2**) that are substituted at the 3-position with either amides, urethanes, or ureas.

Derivatization of aminopyridone **4** to afford intermediate **5** could be achieved directly via treatment with (a) an acyl halide in the presence of a base (method A); (b) a carboxylic acid, a water soluble carbodiimide,[11] 1-hydroxybenzotriazole, and 4-(dimethylamino)pyridine (method B); or (c) an isocyanate and triethylamine (method C). Indirect acylation to afford either urethanes or ureas was also achievable by sequential treatment of the amine with triphosgene and triethylamine followed by the addition of either an alcohol or an amine (method D). Formation of alcohol **6** was accomplished via treatment of pyridones **5** or **3** with buffered tetrabutylammonium fluoride. Oxidation of alcohol **6** to trifluoromethyl ketone **2** was done using a modified Pfitzner–Moffatt procedure.[12]

Although Scheme 1 could be expanded to include the preparation of either 3-alkylamino or 3-sulfonamido substituted pyridone–TFMKs (**10** or **13**, see Scheme 2), this was not the preferred sequence for these compounds. In both of these cases the 3-position NH of the intermediate alcohol (**9** or **12**) was sufficiently acidic that during the Pfitzner–Moffatt oxidation interception of the activated dimethyl sulfoxide by this nitrogen atom occurred with resultant formation of a N-CH_2SCH_3 alkylated side product that could only be removed by tedious chromatography.

As a result we developed an alternate approach to the amino and sulfonamido substituted pyridone–TFMKs (**10** and **13**) (see Scheme 2). This route avoided the use of oxidants late in the sequence and the problematic formation of a N-thiomethylated side product. Starting with pyridone **2a**, hydrogenolysis afforded amino ketone **7** that could be derivatized using the same protocols (methods A, B, C, and D) described above for aminopyridone **3**. Although Scheme 2 is just a reordering of the steps reported in Scheme 1 this route was not initially obvious since in the related peptidic TFMK series the amino ketone corresponding to **7** is unstable due to its greater basicity.[13] Alkylation of amino ketone **7** to afford ethylamine **10** was achieved by treatment with

Scheme 1[a,b]

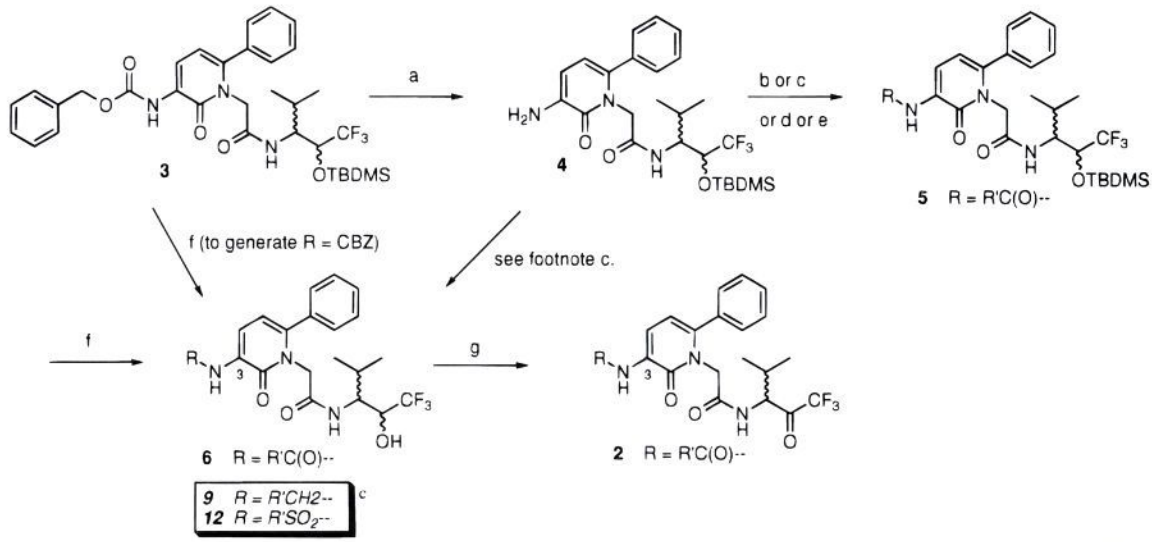

[a] Reagents: (a) H_2, Pd/C, EtOH; (b) Acylation method A: R′COCl, base (*N*-methylmorpholine, pyridine, or triethylamine [TEA]), THF; (c) method D: (i) $(Cl_3CO)_2C{=}O$, TEA, CH_2Cl_2; (ii) R″OH or $R''NH_2$; (d) method C: $R''N{=}C{=}O$, cat. TEA, THF; (e) method B: $R'CO_2H$, WSCDI, HOBT, DMAP, CH_2Cl_2; (f) $Bu_4N^+F^-$, HOAc, THF; (g) 10 equiv of WSCDI, 2 equiv of Cl_2CHCO_2H, DMSO/THF, 0 °C → room temperature. [b]R is defined in Table 2 and the appropriate sequences of compounds are: **3** → **4** → **5** → **6** → **2** or **3** → **6** → **2**. [c]As described in the text compounds **9** and **12** could be similarly prepared from **4** by alkylation/sulfonylation followed by deprotection. However poor yields of the amino or sulfonamido substituted trifluoromethyl ketones after oxidation using condition (g) led to the development of the route illustrated in Scheme 2.

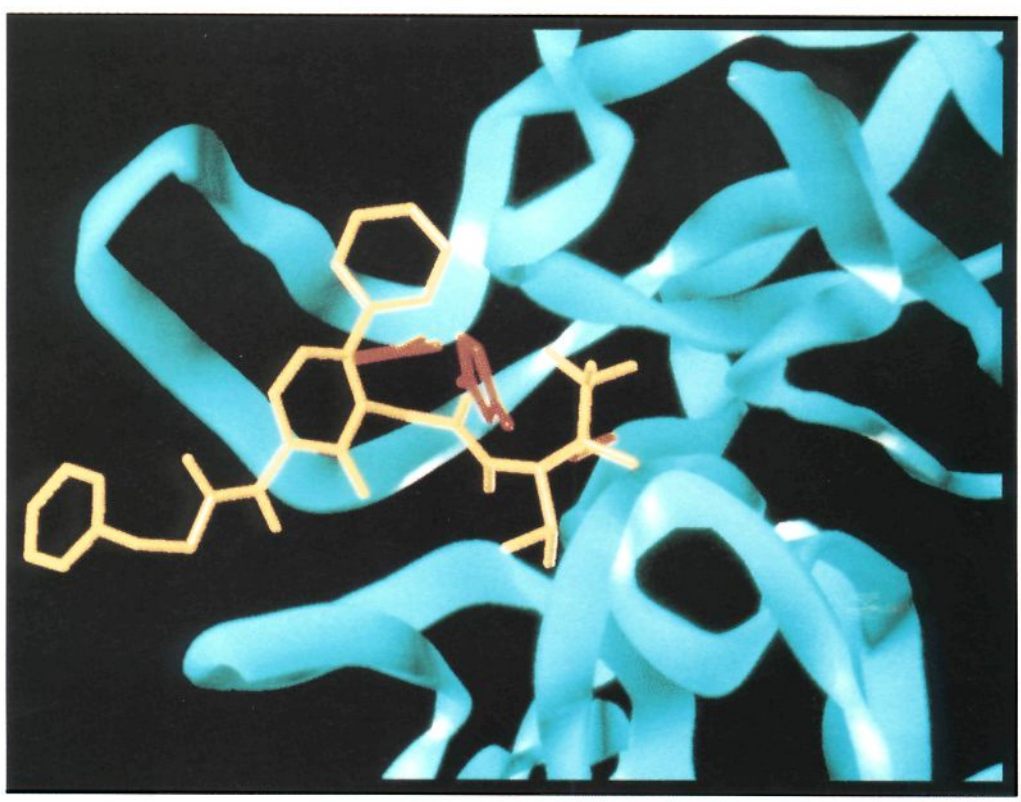

Figure 3. A single-frame "snap shot" of a 40 ps aqueous molecular dynamics simulation of pyridone **2a** (in yellow) bound to HLE (cyan ribbon with the catatlytic triad in red) showing the CBZ group of the inhibitor exposed to the aqueous environment.

ethyl iodide and 2,6-lutidine in DMF at room temperature. Sulfonamidation and sulfamidation were accomplished by treatment of amino ketone **7** with sulfonyl or sulfamoyl chlorides in the presence of 2,6-lutidine.[14]

Further transformation of these inhibitors to the rest of the compounds listed in Table 2 was achieved by the routes illustrated in Schemes 3–5. The pyridine *N*-oxides **2h** and **2i** were prepared (Scheme 3) from the corresponding pyridines **2e** and **2f** by reaction with dimethyldioxirane in acetone.[15] Urea **2v** was prepared from amino ketone **7**, via an unstable *N*-sulfonic acid intermediate (Scheme 4), by sequential treatment with chlorosulfonyl isocyanate and saturated sodium bicarbonate solution.[16]

Carboxylic acids **2j-m** were prepared (Scheme 5) by basic hydrolysis of their corresponding esters with lithium hydroxide in THF/water. Attempted basic

Scheme 2[a,b]

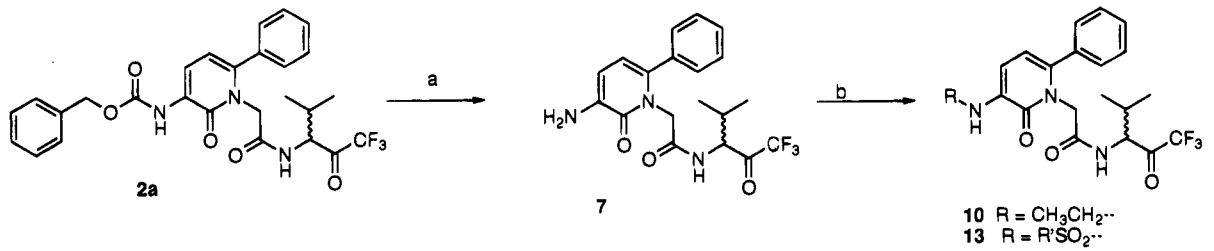

[a] Reagents: (a) H_2, Pd/C, EtOH or trifluoromethanesulfonic acid/anisole; (b) or $R'SO_2Cl$ or $R'CH_2I$, 2,6-lutidine, THF. [b] R is defined in Table 2.

hydrolysis of the methyl ester analog of acid **2n** resulted in attack of the pyridone 3-NH nitrogen on the ester carbonyl to form a homophthalimide. As an alternative, benzyl ester **14n** was prepared and its benzyl group was removed by hydrogenolysis. All of these esters were prepared via Scheme 1 using the appropriate acylating reagent and method A.

Results and Discussion

Biological testing of the compounds listed in Table 2, consisted of (1) evaluation in vitro of the compound's ability to inhibit HLE-catalyzed hydrolysis of MeO-Suc-Ala-Ala-Pro-Ala-pNA, via measurement of the inhibition constant (K_i) by using the published method,[17] and (2) determination of oral efficacy in an in vivo acute hemorrhagic assay (AHA).

Initial studies showed that variation of the 3-position amino substituent could afford inhibitors that retained good in vitro potency (e.g., compare **2b** or **2c** to **2a**). These results supported the above stated hypothesis that in vitro potency could be maintained upon modification of the CBZ group. In contrast, the *p*-methoxybenzamide derivative, **2d**, gave almost a 100-fold increase in K_i, relative to the corresponding CBZ derivative, **2a**. This marked a significant departure from the SAR that had been observed in a related series of peptidic trifluoromethyl ketones (Table 3). In that series, the CBZ (**16**) and *p*-methoxybenzamide (**17**) derivatives showed very similar K_i values.[18] Therefore, while general support for the design hypothesis was indicated, specific examples which resulted in loss of potency were also demonstrated.

These results also appeared to reinforce a modeling-based proposal that 3-(substituted amino)pyridones bind in the active site of the enzyme somewhat differently than do the corresponding peptidic inhibitors. Comparison of modeling-based images of the pyridone and peptidic inhibitors bound in the active site of HLE illustrated the geometric differences between these two inhibitors (Figure 4). In the pyridone series, the planar pyridone ring directs the 3-position nitrogen substituent toward a turn section, containing Gly-218 on the surface of the enzyme. In the peptidic series of inhibitors, the tetrahedral geometry at the P_3 α-carbon directs the amino substituent toward the sterically accommodating S_4 pocket of the enzyme (Figure 4). When pyridones contain the conformationally constrained *p*-methoxybenzamide at the 3-position, molecular modeling suggests that significant steric interactions may prevent efficient hydrogen bond formation between the pyridone and the Val-216 region of the enzyme. This would be expected to result in the observed increase in K_i. More conformationally flexible subsitutents, such as CBZ, do not suffer this fate since their pendant (benzyl) groups can rotate to avoid unfavorable steric interactions.

Combining these initial observations with our goal of increased solubility for the test compounds led to the selection of 3-amino substituents that were both conformationally flexible and that contained solubilizing groups (e.g., carboxylic acids, bases, etc.).

Acidic Aryl-Substituted Compounds. A number of carboxylic acid-containing inhibitors (**2j-n**) were prepared as part of our investigations (Table 2). These compounds were found to have good in vitro potency and substantially increased solubility relative to **2a** at pH 7.4. Despite their increased solubility, most of these compounds were inactive orally when dosed 30 min prior to HLE challenge. Measurement of the solubility of several of these compounds at pH 2, which would more closely mimic conditions in the stomach, showed them to be poorly soluble. Since it is known that some carboxylic acids are preferentially absorbed from the stomach in their unionized form,[19] the poor solubility of the acids under these conditions may act to limit their oral absorption.

Basic and Neutral Aryl-Substituted Compounds. We also prepared a large number of compounds that contained basic substituents at the 3-position. Replacement of the benzyl group in compound **2b** by various pyridylmethyl groups (compounds **2e-g**) resulted in increased aqueous solubility of up to several hundred-fold with only modest increases in K_i. None of these compounds, unfortunately, demonstrated oral activity. Transformation of these pyridines into their *N*-oxides (e.g., **2h** and **2i**) resulted in an increase in aqueous solubility, a decrease of in vitro potency, and modest oral activity for **2h** at 80 mg/kg. Given the increased solubility of the pyridylureas and the oral activity of *N*-oxide **2h,** we prepared pyridyl urethanes **2o** and **2p**. As was the case for the pyridylurea series, these urethanes were equipotent in vitro to the parent phenyl analog, **2a**. However, while they were both thermodynamically and kinetically much less soluble than the ureas, both urethanes were orally active, suggesting that solubility is not the sole criteria for oral activity.

In an effort to understand why structurally similar compounds such as **2o** and **2e** demonstrate such different oral activity, the oral bioavailability of these compounds was measured in the hamster (Table 1). Those studies revealed that while the orally active compound (**2o**) had a 45% bioavailability, the bioavailability of the inactive compound (**2e**) was only ~2%. This suggests that the difference in their oral activity is most likely due to differences in absorption (**2o** > **2e**) when administered orally rather than to differences in their relative solubilities (**2e** > **2o**). Extending the bioavailability

Table 2. HLE Activity, Preparation, and Characterization of Pyridone Trifluoromethyl Ketones[a]

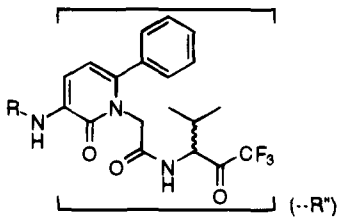

#	R Group	Molecular Formula	Synthetic Route[b]	K_i (nM)[c]	Solubility[d] (mg/mL)	C log P[e]	log P[f]	Oral Activity[g] % inhibition / dose (mg/kg)
2a	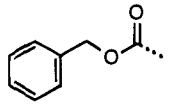	$C_{27}H_{26}F_3N_3O_5$	**1**	4.5±0.8	0.0018	5.12		NS/20
2b	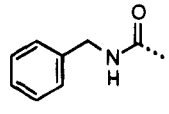	$C_{27}H_{27}F_3N_4O_4 \cdot 1.0\ CH_3CO_2H$	**1/C**	7.0±1.6	ND			not tested
2c	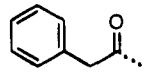	$C_{27}H_{26}F_3N_3O_4 \cdot$	**1 / A**	15.0±2.6	ND			not tested
2d	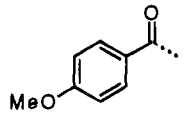	$C_{27}H_{26}F_3N_3O_5 \cdot$	**1/ A**	480.0±170	ND			not tested
2e	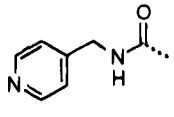	$C_{26}H_{26}F_3N_5O_4$	**1**	16.0±1	0.14	2.98	2.16	NS/60
2f	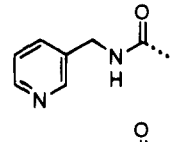	$C_{26}H_{26}F_3N_5O_5 \cdot 0.75\ H_2O$	**1/ D**	15.0±3	0.43	2.98	2.84	NS/40
2g	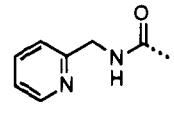	$C_{26}H_{26}F_3N_5O_4$	**1/ D**	15.0±3	0.30	2.98	2.15	NS/20
2h	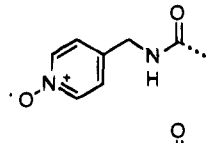	$C_{26}H_{26}F_3N_5O_5 \cdot 0.5\ H_2O$	**3**	52.0±5	1.2	NC	1.13	45/80, NS/20
2i	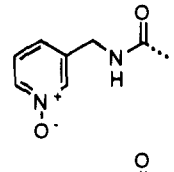	$C_{26}H_{26}F_3N_5O_5 \cdot 1.0\ H_2O \cdot 0.25\ C_3H_8O$	**3**	52.0±1	3.18	NC	1.48	NS/80
2j	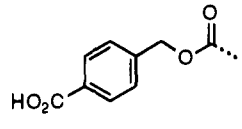	$C_{28}H_{26}F_3N_3O_7$	**5**	5.7±1.5	2.60 [0.0023 at pH 2.0]	4.86	0.84	NS/80
2k	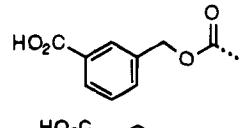	$C_{28}H_{26}F_3N_3O_7$	**5**	4.8±0.8	1.57 [0.014 at pH 2.0]	4.86	ND	NS/80
2l	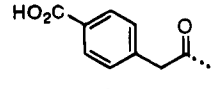	$C_{27}H_{26}F_3N_3O_6$	**5**	13.0±2	2.5	4.26	0.35	NS/40
2m	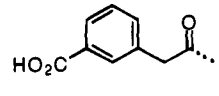	$C_{27}H_{26}F_3N_3O_6$	**5**	23.0±2	0.90	4.26		47/80

Table 2 (Continued)

#	R Group	Molecular Formula	Synthetic Route[b]	K_i (nM)[c]	Solubility[d] (mg/mL)	C log P[e]	log P[f]	Oral Activity[g] % inhibition / dose (mg/kg)
2n	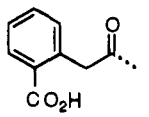	$C_{27}H_{26}F_3N_3O_6 \cdot 0.5\ H_2O$	**5**	18.0±4	2.5	4.26	1.14	NS/80
2o	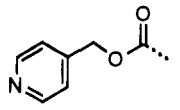	$C_{26}H_{25}F_3N_4O_5 \cdot 0.6\ H_2O$	**1/D**	8.0±1	0.016	3.64	2.41	96/100, 68/80, 59/20, NS/5
2p	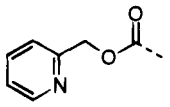	$C_{26}H_{25}F_3N_4O_5 \cdot 0.1\ H_2O$	**1/D**	8.8±1.9	0.0021	3.64	1.91	72/40, NS/20
2q	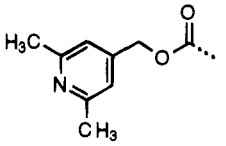	$C_{28}H_{29}F_3N_4O_5 \cdot 1.2\ H_2O$	**1/D**	4.1±2.1	0.0085	4.94	2.38	95/100, 59/20, 42/5, NS/2.5
2r		$C_{21}H_{22}F_3N_3O_4 \cdot 0.2\ H_2O$	**1/A**	57.0±10	0.092	2.75	1.78	48/40, NS/20
2s	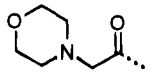	$C_{25}H_{29}F_3N_4O_5 \cdot 0.1\ H_2O$	**1/B**	469.0±190	0.023	2.84	2.00	
2t		$C_{21}H_{19}F_6N_3O_4 \cdot 0.25\ H_2O$	**1/A**	39.0±11	ND	3.86		54/5, NS/2.5
2u		$C_{20}H_{20}F_3N_3O_4$	**1/B**	26.0±3	0.22	2.76	1.84	33/2.5
2v		$C_{20}H_{21}F_3N_4O_4 \cdot 0.25\ H_2O$	**4**	43.0±6	ND	2.44		52/20, NS/5
2w	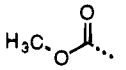	$C_{21}H_{22}F_3N_3O_5$	**1/A**	15.0±3	ND	3.35		NS/2.5
2x	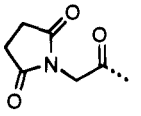	$C_{21}H_{22}F_3N_3O_4 \cdot 0.2\ H_2O$	**1/B**	30.0±7	3.1	1.20	0.96	NS/40
2y	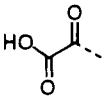	$C_{21}H_{20}F_3N_3O_6 \cdot 0.50\ H_2O$	**5**	34.0±15	ND	NC		55/20, NS/5
2z	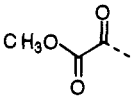	$C_{22}H_{22}F_3N_3O_6 \cdot 0.25\ H_2O$	**1/A**	80.0±30	0.84	NC		NS/20
7		$C_{19}H_{20}F_3N_3O_3 \cdot 0.25\ H_2O$	**2**	62.0±6	0.49	2.51	1.74	65/2.5 @ 30', NS/2.5 @90'
10	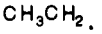	$C_{21}H_{24}F_3N_3O_3$	**2/A**	8.7±3.7	0.28	3.76	2.37	NS/5
13a		$C_{20}H_{22}F_3N_3O_5S$	**2/A**	9.3±4.5	4.1	2.35	1.77	99/100, 58/20, NS/5
13b		$C_{20}H_{19}F_6N_3O_5S$	**2/A**	190.0±90	0.94	4.46	0.94	NS/2.5
13c		$C_{19}H_{21}F_3N_4O_5S \cdot 0.25\ H_2O$	**2/A**	71.0±42	ND	2.01	1.17	NS/20
13d	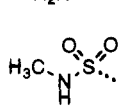	$C_{20}H_{23}F_3N_4O_5S$	**2/A**	18.0±3	1.73	NC	1.79	43/5, NS/2.5

Table 2 (Continued)

#	R Group	Molecular Formula	Synthetic Route[b]	K_i (nM)[c]	Solubility[d] (mg/mL)	C log P[e]	log P[f]	Oral Activity[g] % inhibition / dose (mg/kg)
13e	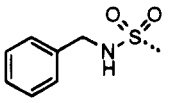	$C_{26}H_{27}F_3N_4O_5S \cdot 0.25\ H_2O$	**2**/A	1.8±0.7	0.021	NC	2.57	43/5, 35/2.5
13f	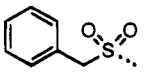	$C_{26}H_{26}F_3N_3O_5S$	**2**/A	1.4±0.2	ND	4.10	ND	55/2.5 @30' NS/2.5 @90'
13g	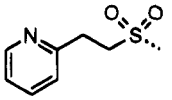	$C_{26}H_{27}F_3N_4O_5S \cdot 0.3\ CH_3OC(CH_3)_3$	**2**/A	6.9±1.7	0.1	2.97		43/20, NS/5
13h	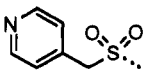	$C_{25}H_{25}F_3N_4O_5S \cdot 1.0\ H_2O$	**2**/A	13.0±5				NS/2.5
13i	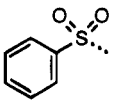	$C_{25}H_{24}F_3N_3O_5S$	**2**/A	6.0±2	0.18	4.01	2.53	85/20, NS/5
13j	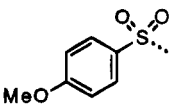	$C_{26}H_{26}F_3N_3O_6S \cdot 0.25\ H_2O$	**2**/A	8.4±3.3		4.10	2.50	35/20, NS/5
13k	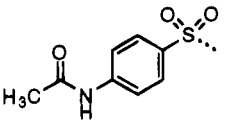	$C_{27}H_{27}F_3N_4O_6S \cdot 1.0\ H_2O$	**2**/A	0.7±0.2	ND		ND	NS/2.5
13l	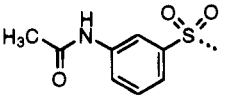	$C_{27}H_{27}F_3N_4O_6S \cdot 0.5\ H_2O$	**2**/A	9.4±4.7				NS/2.5 @90'

[a] Abbreviations are defined in ref 2. [b] The synthetic route is indicated by reference to the Scheme describing it/followed by the acylation method (if any) used. If in bold indicates that it is included as an example in the Experimental Section. [c] The inhibition constant (K_i) versus HLE was determined using the method described in ref 16. [d] Solubility of the compound in 0.01 M sodium phosphate buffer at pH = 7.4. [e] Calculated using CLOGP3 v3.4, MedChem Software, Daylight Chemical Information Systems, 2 Corporate Park, Suite 204, Irvine, CA 92714. [f] Partition coefficients were determined by the Zeneca Structural Chemistry Group using octanol/water in a standard shake-flask protocol as described by Leo, A.; Hansch, C.; Elkins, D. Partition Coefficients and Their Uses. *Chem. Rev.* **1991**, *71*, 525–616. [g] Percent inhibition of elastase-induced lung hemorrhage when the compound is dosed orally at the indicated dose. All reported % inhibition reflect statistically significant ($P < 0.05$ using the standard students T test) difference from the controls. Due to the variability of this assay compounds active (at <95% inhibition levels) were tested at least two separate times. Only if two or more studies showed significant inhibition was the compound considered orally active and then the % inhibition reported is the average of the individual values. Unless otherwise stated the compound was dosed 30 min prior to instillation of HLE.

Scheme 3[a,b]

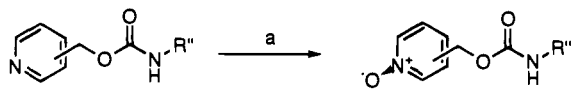

2e, 2f **2h, 2i**

[a] Reagents: (a) dimethyldixoirane, acetone. [b]Structure of R'' defined in Table 2.

Scheme 4[a,b]

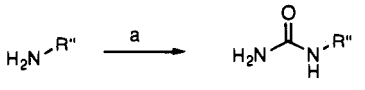

7 **2v**

[a] Reagents: (a) (i) $ClSO_2N{=}C{=}O$, THF; (ii) saturated $NaHCO_3$. [b]Structure of R'' defined in Table 2.

studies with **2o** to dog resulted in the finding that in this species its bioavailability is essentially 100%.

We noted the relatively short $t_{1/2}$ values for **2o** (Table 1) and thought that if the $t_{1/2}$ could be increased while the bioavailability and in vitro potency were retained,

Scheme 5[a,b]

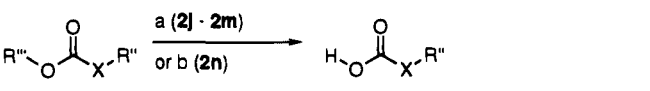

14 **2j - 2n** X = $C_6H_4CH_2$ or $C_6H_4CH_2O$

R''' = Me (**j - m**),
R''' = $PhCH_2$ (**n**)
X = $C_6H_4CH_2$ or $C_6H_4CH_2O$

[a] Reagents: (a) LiOH, THF/H_2O; (b) H_2, 10% (w/w) Pd/C, MeOH. [b]Structure of R'' defined in Table 2.

we might be able to prepare an analog with improved oral potency. Upon the presumption that the pyridyl ring of **2o** might be a target for metabolic degradation we prepared the 2,6-dimethylpyridyl analog, **2q**. These methyl substituents were expected to block metabolic conversion to the *N*-oxide, and we were pleased to find that although this analog showed similar in vitro potency to **2o**, it did have slightly greater in vivo potency.

Aliphatic-Substituted Compounds. We inter-

Table 3. In Vitro Comparison of Peptides to Pyridones

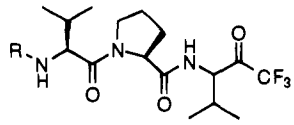

Peptides

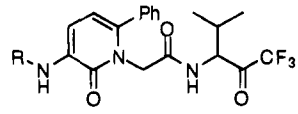

Pyridones

R	K_i (nM) HLE[a] peptide (no.)[b]	K_i (nM) HLE[a] pyridone (no.)
CBZ	2.5 ± 0.3 (**16**)	4.5 ± 0.8 (**2a**)
4-$CH_3OC_6H_4C(O)$	3.1 ± 0.8 (**17**)	480 ± 170 (**2d**)

[a] The K_i was determined using the method described in ref 16. [b] The specific compound number is indicated in parentheses.

preted the small effect that changing the position of the aryl substituent had on in vitro potency (compare **2f/2g**, **2h/2i**, and **2j/2k**) as evidence that our design hypothesis was valid and that the CBZ phenyl ring does not interact strongly with the enzyme. This became particularly important as we assessed whether decreasing the molecular weight of our inhibitors, via removal of the bulky aryl group, would have a favorable impact on oral activity. To do this we prepared several compounds that contained small aliphatic groups as 3-amino substituents. The in vitro potency of acetamide **2r** was approximately 10-fold less than the CBZ derivative **2a**. However, this compound was much more soluble (50-fold) than **2a** and was orally active at 40 mg/kg. Oral bioavailability of **2r** was found to be 35% in the hamster. Replacement of the acetamide with several closely related groups, e.g., **2t**, **2v**, or **2w**, resulted in similar potency in vitro and improved oral activity for the trifluoroacetamide **2t**.

As had been the case with the pyridyl derivatives, improvement of solubility at a given level of in vitro potency was not a sufficient criteria for achieving oral activity. This is illustrated by **2x**, in which a succinimidyl moiety is appended to the acetyl group. Although **2x** retained equivalent in vitro activity to **2r** and was much more soluble, it was inactive upon oral administration at 40 mg/kg. Replacement of the succinimidyl group with a weakly-basic *N*-morpholinyl group (pK_a of the conjugate acid < 7.0) resulted in analog **2s** that showed a surprisingly large increase in K_i.[20]

On the basis of interesting findings that have been previously reported,[1b] oxalate **2y** and oxalate methyl ester **2z** were prepared. Although in vitro these compounds were respectively 6- and 16-fold weaker than **2a**, in vivo oxalate **2y** was active at 20 mg/kg. These results contrast with the earlier findings in the unsubstituted pyridone or 5-benzylpyridone series in which such oxalic acid derivatives were approximately equipotent in vitro with the corresponding CBZ analogs. This suggested that there may be minor differences in the binding modes for these inhibitors that vary according to the substituent pattern of the pyridone nucleus. Decreasing the size of the carbonyl substituent yielded formamide **2u**. This compound, although only slightly more potent in vitro than **2r**, was excitingly one of the first analogs to show po activity at 2.5 mg/kg.

The initial impetus for preparation of the parent amine **7** had been its use as a synthetic intermediate. However, pharmacologic testing showed that it retained equivalent in vitro activity to **2r** and was much more potent in vivo, with po activity at 2.5 mg/kg. The level of in vivo activity for this nonbasic amine (pK_b of 1.90) prompted oral testing following a 3-fold longer, 90 min, prechallenge interval, at which point the compound was found to be inactive. Increasing the lipophilicity of this amine by adding an alkyl substituent, e.g., ethylamine **10**, resulted in a lower K_i value but decreased oral potency.

Sulfonamides. Further variation of the N-substituent provided a number of compounds in which the 3-position amide carbonyl, present in inhibitors such as **2r**, was replaced with other electron-withdrawing groups. One of the first such compounds, methyl sulfonamide **13a**, proved more potent both in vitro and in vivo than **2r**. Although increased solubility had been predicted, neither the magnitude of the difference in solubility (50-fold) nor the better in vitro activity had been anticipated. Previous experience in the R-Val-Pro-Val-TFMK series of HLE inhibitors had shown that P_4-sulfonamides (R = $R'SO_2$) were generally either equipotent to or less potent than the corresponding carboxamides (R = R'C(O)).[13] We attributed this variance in SAR to a combination of the previously discussed difference in binding geometry for the pyridones and the peptides and the different geometries presented by the tetrahedral sulfonyl group and the trigonal amide carbonyl group. These differences might result in sulfonyl and acyl substituents probing different regions of the enzyme's surface.

An ENIGMA-based examination of methyl sulfonamide **13a** and acetamide **2r**, both as isolated compounds and bound to HLE, revealed that the methyl substituent on the sulfonyl group, unlike the acetyl group, could readily rotate away from a coplanar orientation with the 3-position NH. When **13a** was docked into HLE and the resulting complex energy minimized, the C—S—N—H dihedral angle was found to be ~130°. This orientation allows the sulfonamide substituent to move away from the surface of the enzyme, while the pyridone 3-position N-H remains relatively close to the C=O of Val-216. Support for the concept that SO_2 substituents exist in such a rotated geometry when bound to HLE was subsequently obtained by X-ray crystallographic analysis (see discussion below) of one of these sulfonyl-linked inhibitors bound to the related enzyme, PPE.

This difference in binding orientation prompted us to determine and compare the relative enzyme selectivities of sulfonamide **13a** and acetamide **2r**. Previously, the CBZ derivative **2a** had been found to have considerable affinity for bovine pancreatic chymotrypsin (BPC)[1c]—its selectivity ratio (BPC K_i/ HLE K_i) was only 12. Although the selectivity ratio for acetamide **2r** remained low at 21, the ratio for sulfonamide **13a** improved to 612. The overall results obtained with **13a** prompted further exploration of the SARs in the 3-aminosulfonyl substituted pyridones.

Formation of the triflamide **13b** resulted in a 20-fold decrease in potency relative to **13a**. This decrease could be due to the fact that the triflamide N-H is sufficiently acidic (pK_a = 4.02) to be deprotonated under the assay conditions (pH 7.6). Deprotonation would leave the inhibitor unable to form the requisite hydrogen bond with the carbonyl of Val-216.

Several homologous sulfamides, e.g., **13c**, **13d**, and **13e**, were prepared. In contrast to our results for aryl-substituted urethanes, ureas, and amides, these sulfonyl derivatives showed a direct correlation between the

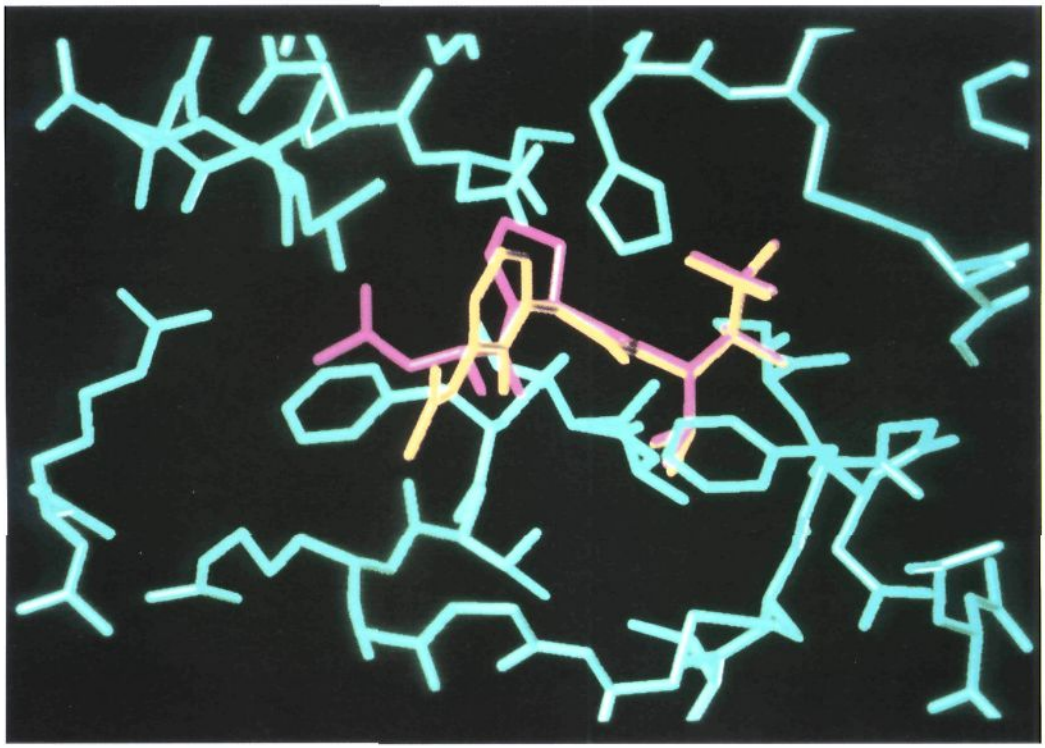

Figure 4. Modeling overlay of an early *N*-acetyl (6-hydrido) pyridone inhibitor (in yellow) onto the peptidic inhibitor, acetyl-Ala-Pro-Val-TFMK (in purple), docked into the active site of HLE (in cyan). Comparison of peptide and pyridone geometry.

lipophilicity of their 3-amino substituent (as estimated by their respective log *P* values of 1.2, 1.8, and 2.6) and their pK_i values (7.1, 7.7, and 8.7). Such a correlation might be expected if the substituent bound in the S_4 pocket of the enzyme. It was also interesting that, qualitatively, the level of in vivo activity of these three compounds was **inversely correlated** with both inhibitor log *P* and solubility.

Support for the idea that the alkyl sulfonamides had better profiles than their corresponding carboxamides was provided by benzyl sulfonamide **13f**. It was 10-fold more potent in vitro than amide **2c** and was also orally active at 2.5 mg/kg. In contrast to the carbonyl derived compounds, attempts to further increase oral activity by replacing the phenyl group with a pyridyl group were unsuccessful in the sulfonyl-linked series. For example, 4-pyridylmethyl sulfonamide **13h** was 10-fold weaker in vitro and also less potent in vivo than tolyl sulfonamide **13f**. Similarily, the pyridylethyl sulfonamide **13g** was weaker both in vitro and in vivo than its related benzyl sulfamide **13e**.

The different geometry around the SO_2—NH bond as compared to the CO—NH bond also suggested the possibility of phenyl sulfonamide derived inhibitors. Such compounds were important to test some design concepts based on either modeling or the SAR previously found in the peptidyl-TFMK series. First, in contrast to the benzamide-substituted pyridones (e.g., **2d**), pyridones substituted with phenyl sulfonamides should not produce an unfavorable steric interaction between the aryl group and enzyme. This is because both the SO_2—NH and the Ph—SO_2 bonds are less geometrically constrained (see above) than the corresponding acyl bonds. The encouraging profile of these types of compounds was demonstrated with sulfonamide **13j**, which was much more potent in vitro than *p*-methoxybenzamide **2d** and was active when administered orally at 20 mg/kg.

Second, molecular mechanics calculations indicated that the terminal carbonyl *oxygen* of a *p*-$CH_3C(O)$-$NHC_6H_4SO_2$-substituted pyridone (**13k**) could reach the N-H of Gly-218, allowing for the formation of a hydrogen bond. Further, aqueous molecular dynamics simulations on **13k** in HLE revealed that this interaction should form and would be stable under aqueous conditions. Confirmation of these modeling-based hypotheses was provided by in vitro testing of **13k** that showed it to be ~10-fold more potent than either **13i** or **13j**. Further support that this increased potency was due to a specific H-bond between HLE and **13k** was indicated by the 20-fold difference in potency found between **13k** and its isomer **13l**. By contrast, the acyl-substituted pyridones show no evidence of such a specific binding interaction, as evidenced by the similar K_i values of each compound in the two sets of isomeric pyridylmethyl (**2e-g**) or toluic acid (**2l-n**) derivatives. The potency of **13k** prompted measurement of its activity against BPC and human chymotrypsin. The selectivity ratios versus HLE, ~3700 and ~9700, respectively, demonstrated that with appropriate N-substituents, these pyridones could provide selective inhibitors. In contrast, to these exciting results in vitro, sulfonamide **13k** showed no significant oral activity, at a dose of 2.5 mg/kg.

X-ray Crystallographic Analysis

Physical support for the modeling-based design hypotheses described above was achieved by X-ray crystallography as exemplified by the following analysis of the complex formed between inhibitor **13d** and PPE.[21]

A crystallography-derived plot of the inhibitor in the active site of the enzyme is shown in Figure 5. The structure obtained agreed closely with that predicted by molecular modeling studies (the predicted interactions are highlighted in this figure). The inhibitor is covalently bound to the enzyme; the bond length of this

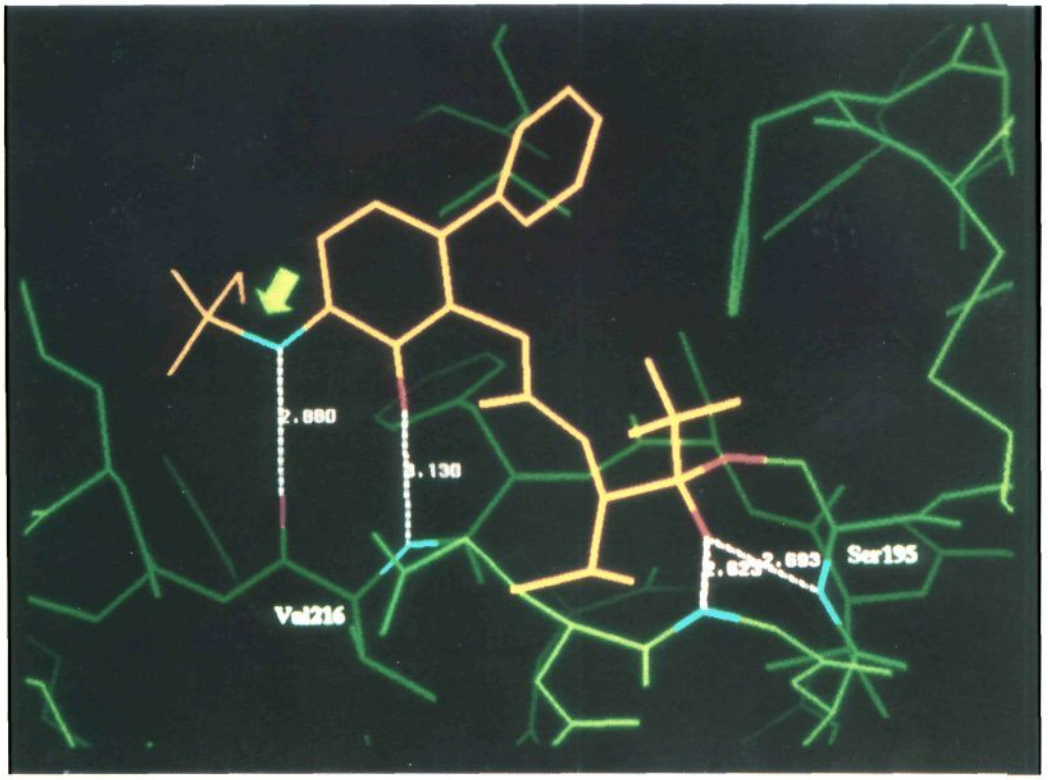

Figure 5. X-ray crystallographic structure of pyridone **13d** (in yellow) complexed to PPE (in green) with the key interacting nitrogen (blue) and oxygen (red) atoms highlighted and the measured interatomic distances for the predicted H-bonds displayed.

hemiketal linkage between the inhibitor's carbonyl carbon and Oγ of Ser-195 is 1.45 Å. The carbonyl carbon is tetrahedral. The hemiketal oxygen atom is pointing toward the oxyanion hole[22] and is within hydrogen bonding distance of the amido nitrogen atoms of Gly-193 (2.62 Å) and Ser-195 (2.69 Å). A pair of β-sheet hydrogen bonds is observed between the pyridone carbonyl oxygen and the amido nitrogen of Val-216 (3.13 Å) and the pyridone 3-amino nitrogen and the carbonyl oxygen of Val-216 (2.88 Å). The isopropyl group of the inhibitor is found in the S_1 pocket of the enzyme, while the 6-phenyl substituent of the pyridone is in the S_2 pocket. The geometry of the pyridone 3-sulfamoyl substituent is such that the torsion angle $C_{3(\text{pyridone})}$—N—S—N is 73°.

Additional close contacts involving inhibitor, enzyme, and solvent are also observed (not highlighted in Figure 5). The P_1—P_2 amido nitrogen of the inhibitor makes a hydrogen bond with the carbonyl oxygen of Ser-214 (3.16 Å). An oxygen in the sulfonyl group is accepting a hydrogen bond from the amido nitrogen of Arg-217A (3.18 Å). An active-site water molecule is involved in a pair of interactions bridging ligand and enzyme. This water molecule is within hydrogen bonding distance of the pyridone carbonyl oxygen (2.95 Å) and Nϵ of Gln-192 (3.02 Å). The plane defined by these latter two interactions is roughly at right angles to the plane of the β-sheet.

Summary

These studies demonstrate the utility of molecular modeling in the exploration of a series of pyridone-based inhibitors of HLE. Physicochemical, pharmacokinetic, and pharmacologic analysis of **2a** had led to the hypothesis that poor physical properties were the basis for its lack of efficacy in vivo. Modeling was used to predict where changes to **2a** could be made that would effect physical properties but that would allow retention of intrinsic in vitro activty. A crystal structure of **13d** with PPE experimentally supports the modeling-based proposal for the mode of binding for these inhibitors. In general, the results obtained indicate that both in vitro and in vivo activity could be retained over a wide range of inhibitor solubilities and log P values. In particular, starting with pyridone **2a**, optimization of the 3-amino substituent resulted in analogs that showed (a) an significant increase in potency against in vitro HLE (e.g., **13k**) and (b) oral inhibition of HLE-induced hemorrhage, with activity at 2.5 mg/kg (e.g., **2u**, **7**, **13e**, and **13f**). Further improvement in the oral profile (extending the duration of action) of these inhibitors required altering the pyridone nucleus and will be discussed in a subsequent paper.[23]

Experimental Section

General Methods. Proton NMR (NMR) spectra were recorded on either a Bruker WM 250 (250 MHz) or Bruker WM 300 (300 MHz) instrument in DMSO-d_6, except where indicated. Chemical shifts are reported in parts per million (δ) relative to internal tetramethylsilane. Peaks are reported as s, singlet; d, doublet; t, triplet; b, broad; ex, exchanged by added deuteriotrifluoroacetic acid or D_2O. Mass spectra (CIMS) were recorded on a Kratos MS-80 instrument or Finnigan MAT-60 operating in the chemical ionization mode using methane as reagent gas. Melting points were determined on a Thomas-Hoover capillary melting point apparatus and are uncorrected. Combustion analyses for carbon, hydrogen, and nitrogen were performed on a Perkin-Elmer 241 instrument by the Analytical Section, Zeneca Pharmaceutical Group, and are within ±0.4% of theoretical values. Flash chromatography[24] was performed using the indicated solvent ratios (v/v) on Kieselgel 60 (230–400 mesh) supplied by E. Merck. Analytical thin-layer chromatography (TLC) was conducted either on prelayered silica gel GHLF 250 μm plates (Analtech, Newark, DE) or on Whatman $MKC_{18}F$ 200 μm

reversed-phase TLC plates (RP-TLC). Visualization of the plates was effected by using UV light and/or phosphomolybdic acid–sulfuric acid charring. Tetrahydrofuran (THF) was distilled from sodium–benzophenone ketyl; dichloromethane, pyridine, *N,N*-dimethylformamide (DMF), and dimethyl sulfoxide (DMSO) were distilled from calcium hydride. All other reagents were purified by standard methods (recrystallization or distillation) as needed. All organic solutions were dried (with anhydrous magnesium sulfate unless indicated otherwise) prior to concentration.

Synthesis of 2a: Example Of Sequence 3 → 6a → 2a. 2-[3-[(Benzyloxycarbonyl)amino]-2-oxo-6-phenyl-1,2-dihydro-1-pyridyl]-*N*-(3,3,3-trifluoro-2-hydroxy-1-isopropylpropyl)acetamide (6a). General Procedure a: Removal of the TBDMS Group (Scheme 1, Reagent f). A solution 2-[3-[(benzyloxycarbonyl)amino]-2-oxo-6-phenyl-1,2-dihydro-1-pyridyl]-*N*-[2-[(*tert*-butyldimethylsilyl)oxy]-3,3,3-trifluoro-1-isopropylpropyl]acetamide (**3**) (0.96 g, 1.49 mmol) in tetrahydrofuran (8 mL) was treated with tetrabutylammonium fluoride (1 M in tetrahydrofuran; 1.62 mL, 1.62 mmol), and the mixture was stirred for 4.5 h. The reaction mixture was diluted with ethyl acetate (75 mL), washed with water (twice) and brine, dried, and evaporated to yield a yellow foam. Purification by flash chromatography, eluting with ethyl acetate:chloroform (first 5:95, then 10:90), and overnight drying under vacuum gave **6a** as a white solid (0.793 g) in quantitative yield: TLC R_f = 0.19, chloroform:ethyl acetate (20:1); NMR δ 0.81 (d, 3, J = 6.7 Hz), 0.88 (d, 3, J = 6.7 Hz), 1.67–1.84 (m, 1), 3.82 (t, 1, J = 8.8 Hz), 4.0–4.17 (m, 1), 4.34 (d, 1, J = 15 Hz), 4.50 (m, 1), 5.18 (s, 2), 6.20 (d, 1, J = 7.7 Hz), 6.49 (d, 1, J = 7 Hz), 7.31–7.47 (m, 10), 7.86 (d, 1, J = 9.7 Hz), 7.91 (d, 1, J = 7.7 Hz), 8.53 (s, 1); MS m/z = 532 (M + 1).

2-[3-[(Benzyloxycarbonyl)amino]-2-oxo-6-phenyl-1,2-dihydro-1-pyridyl]-*N*-(3,3,3-trifluoro-1-isopropyl-2-oxopropyl)acetamide (2a). General Procedure b: Oxidation of Alcohol (Scheme 1, Reagent g). A solution of **6a** (0.78 g, 1.47 mmol) in dimethyl sulfoxide (4 mL) and toluene (4 mL) was treated with 1-[3-(dimethylamino)propyl]-3-ethylcarbodiimide hydrochloride (2.81 g, 14.7 mmol) and dichloroacetic acid (0.48 mL, 3.72 mmol). After stirring overnight, the reaction mixture was diluted with ethyl acetate (100 mL), washed successively with 10% hydrochloric acid (twice), saturated aqueous sodium bicarbonate (twice) and brine, dried, and evaporated to give an off-white solid (0.75 g). Flash chromatography, eluting with dichloromethane:ethyl acetate (95:5), and drying overnight in a vacuum oven gave **2a** as an off-white solid (0.53 g, 68% yield): TLC R_f = 0.29, dichloromethane:ethyl acetate (20:1); NMR δ 0.83 (d, 3, J = 6.8 Hz), 0.89 (d, 3, J = 6.7 Hz), 2.10–2.21 (m, 1), 4.46 (d, 1, J = 16 Hz), 4.54 (d, 1, J = 16 Hz), 4.63 (t, 1, J = 6 Hz), 5.19 (s, 2), 6.23 (d, 1, J = 7.6 Hz), 7.33–7.49 (m, 10), 7.92 (d, 1, J = 7.6 Hz), 8.55 (s, 1), 8.74 (d, 1, J = 7.0 Hz); MS m/z = 530 (M + 1).

Synthesis of 2b: Example of Sequence 4 → 5b → 2b. 2-[3-[(Benzylureido)-2-oxo-6-phenyl-1,2-dihyro-1-pyridyl]-*N*-(2-[(*tert*-butyldimethylsilyl)oxy]-3,3,3-trifluoro-1-isopropylpropyl]acetamide (5b). Method C: Acylation Using an Isocyanate (Scheme 1, Reagent d). To a solution of 2-(3-amino-2-oxo-6-phenyl-1,2-dihydro-1-pyridyl)-*N*-[2-[(*tert*-butyldimethylsilyl)oxy]-3,3,3-trifluoro-1-isopropylpropyl]acetamide (**4**) (300 mg, 0.59 mmol) in tetrahydrofuran (10 mL) was added benzyl isocyanate (86 mg, 0.65 mmol). After 20 h triethylamine (65 mg, 0.64 mmol), and benzyl isocyanate (43 mg, 0.32 mmol) were added. After another 18 h the reaction mixture was diluted with ethyl acetate and 10% hydrochloric acid. The organic portion was separated, washed with 10% hydrochloric acid and brine, and evaporated to give a crude oil. The reaction was found to be incomplete. To a solution of the recovered oil in tetrahydrofuran (6 mL) was added triethylamine (80 mg, 0.79 mmol) and benzyl isocyanate (86 mg, 0.64 mmol). The solution was heated under reflux for 6 h and stirred for 18 h. The reaction mixture was diluted with ethyl acetate, washed with saturated aqueous sodium bicarbonate, 10% hydrochloric acid and brine, dried, evaporated, and dried under vacuum to give a crude solid. Purification by chromatography, eluting with ethanol:ethyl acetate:dichloromethane (0.25:3:96.75), gave **5b** (295 mg, 78% yield): TLC R_f = 0.20, ethanol:ethyl acetate:dichloromethane (0.5:4:95.5); NMR (partial) δ 0.098 (d, 6, J = 4.5 Hz), 0.74–1.0 (m, 15), 1.63 –1.84 (m, 1), 3.83 (t, 1, J = 9.3 Hz), 4.30 (d, 2, J = 7 Hz), 4.58 (d, 1), 6.16 (d, 1, J = 7.5 Hz), 7.17–7.20 (m, 11), 8.09 (d, 1, J = 7.5 Hz), 8.48 (d, 1); MS m/z = 645 (M + 1).

2-[3-(Benzylureido)-2-oxo-6-phenyl-1,2-dihydro-1-pyridyl]-*N*-(3,3,3-trifluoro-1-isopropyl-2-oxopropyl)acetamide (2b). Using general oxidation procedure b, compound **2b** was prepared by oxidation of the corresponding alcohol **6b** and was isolated in 34% yield after chromatography using acetic acid:ethyl acetate:dichloromethane (0.5:10:89.5) as eluent: TLC R_f = 0.23, acetic acid:ethyl acetate:dichloromethane (0.5:10:89.5); NMR δ 0.805 (d, 3, J = 6.9 Hz), 0.865 (d, 3, J = 6.9 Hz), 1.93 (s, 2, two overlapping singlets), 2.17–2.34 (m, 1), 4.07 (d, 1, J = 3 Hz), 4.31 (s, 2), 4.48 (AB q, 2, J = 28.5 Hz), 6.18 (d, 1, J = 9 Hz), 7.05–7.20 (m, 10), 8.07 (dd, 1, J = 7.5, 7.8 Hz); MS m/z = 529 (M + 1).

Synthesis of 2c: Example of Sequence 3 → 4 → 5c → 6c → 2c. 2-[3-Amino-2-oxo-6-phenyl-1,2-dihydro-1-pyridyl)-*N*-(2-[(*tert*-butyl-dimethylsilyl)oxy]-3,3,3-trifluoro-1-isopropylpropyl]acetamide (4). General Procedure c: Hydrogenolytic Removal of the CBZ Group (Scheme 1, Reagent a). To a solution of 2-[3-[(benzyloxycarbonyl)-amino]-2-oxo-6-phenyl-1,2-dihydro-1-pyridyl]-*N*-[2-[(*tert*-butyldimethylsilyl)oxy]-3,3,3-trifluoro-1-isopropylpropyl]acetamide (**3**) (2.41 g, 3.7 mmol) in tetrahydrofuran (8 mL) was added 10% (w/w) palladium-on-carbon (0.50 g) in tetrahydrofuran (8 mL) under nitrogen. This mixture was stirred under hydrogen at atmospheric pressure for 5 h. The catalyst was removed by filtration through a plug of diatomaceous earth, and the plug was washed with ethanol. The filtrate was evaporated and dried under vacuum to give **4** (1.78 g, 95% yield): TLC R_f = 0.06, ethyl acetate:dichloromethane (6:94); NMR δ 0.11 (d, 6, J = 4.5 Hz), 0.77–1.10 (m, 15), 1.59–1.91 (m, 1), 3.84 (t, 1, J = 7.5 Hz), 4.28 (d, 1, J = 7.5 Hz), 4.42 (d, 1, J = 15 Hz), 4.69 (d, 1, J = 17.5 Hz), 6.31 (d, 1, J = 7.5 Hz), 7.62–7.85 (m, 6); MS m/z = 512 (M + 1).

***N*-[2-[(*tert*-Butyldimethylsilyl)oxy]-3,3,3-trifluoro-1-isopropylpropyl]-2-[2-oxo-6-phenyl-3-[(phenylacetyl)amino]-1,2-dihydro-1-pyridyl]acetamide (5c). Method A: Acylation Using an Acid Chloride (Scheme 1, Reagent b).** A 25 mL flask under nitrogen was charged with **4** (0.301 g, 0.59 mmol) dissolved in tetrahydrofuran (6 mL). Triethylamine (0.09 mL, 0.64 mmol) was added, followed by phenylacetyl chloride (0.08 mL, 0.6 mmol). The cloudy, yellow solution was stirred overnight; diluted with ethyl acetate (50 mL), washed with 10% hydrochloric acid (three times), saturated aqueous sodium bicarbonate (three times), and brine, dried, and evaporated to give an oil that solidified under vacuum. The solid was purified by chromatography, eluting with ethyl acetate:dichloromethane (3:97), to afford **5c** (0.272 g, 74% yield): TLC R_f = 0.54, methanol:dichloromethane (1:99); NMR (DMSO–TFAd) δ 0.115 (d, 6, J = 4.5 Hz), 0.8–1.0 (m, 15), 1.63–1.87 (m, 1), 3.86 (s, 2), 4.27 (q, 1, J = 9 Hz), 4.34–4.47 (d, 1), 4.56–4.73 (br d, 1), 6.19 (d, 1, J = 7.2 Hz), 7.20–7.53 (m, 10), 7.63 (d, 1, J = 7.5 Hz), 8.32 (d, 1, J = 7.5 Hz); MS m/z = 630 (M + 1).

2-[2-Oxo-6-phenyl-3-[(phenylacetyl)amino]-1,2-dihydro-1-pyridyl]-*N*-(3,3,3-trifluoro-2-hydroxy-1-isopropylpropyl)-acetamide (6c). Using a similar procedure to that described in general procedure a for the removal of TBDMS groups, except for diluting the reaction mixture with ethyl acetate, washing it with water, and evaporating it, *N*-[2-[(*tert*-butyldimethylsilyl)oxy]-3,3,3-trifluoro-1-isopropylpropyl]-2-(2-oxo-6-phenyl-3-[(phenylacetyl)amino]-1,2-dihydro-1-pyridyl)-acetamide (**5c**) was converted into 2-[2-oxo-6-phenyl-3-[(phenylacetyl)amino]-1,2-dihydro-1-pyridyl]-*N*-(3,3,3-trifluoro-2-hydroxy-1-isopropylpropyl)acetamide (**6c**): TLC R_f = 0.23, methanol:dichloromethane (1:99); NMR (DMSO–TFAd) δ 0.813 (d, 3, J = 6.5 Hz), 0.88 (d, 3, J = 6.75 Hz), 1.63–1.87 (m, 1), 3.82 (s, 2), 4.07 (q, 1, J = 7.25 Hz), 4.45 (q, 2, J = 27.5 Hz), 6.17 (d, 1, J = 7.5 Hz), 7.17–7.53 (m, 10), 7.83 (d, 1, J = 7.5 Hz), 8.27 (d, 1, J = 7.5 Hz); MS m/z = 516 (M + 1).

2-[2-Oxo-6-phenyl-3-[(phenylacetyl)amino]-1,2-dihydro-1-pyridyl]-*N*-(3,3,3-trifluoro-1-isopropyl-2-oxopropyl)-acetamide (2c). Using a similar procedure to that described in general oxidation procedure b but using methanol:dichlo-

romethane (1:99) as the chromatography solvent, **6c** was oxidized to afford **2c**: NMR δ 0.71–0.94 (m, 6), 2.06–2.30 (m, 1), 3.8 (s, 2), 4.50 (q, 2, J = 6.75 Hz), 4.63 (t, 1, J = 5 Hz), 6.19 (d, 1, J = 7.5 Hz), 7.17–7.53 (m, 10), 8.27 (d, 1, J = 7.5 Hz), 8.73 d, 1, J = 7.5 Hz), 9.46 (s, 1); MS m/z = 514 (M + 1).

2-[2-Oxo-[3-[(1-oxopyrid-4-yl)methyl]ureido]-6-phenyl-1,2-dihydro-1-pyridyl]-*N*-(3,3,3-trifluoro-1-isopropyl-2-oxopropyl)acetamide (2h). A solution of 2-[2-oxo-6-phenyl-3-[3-(4-pyridylmethyl)ureido]-1,2-dihydro-1-pyridyl]-*N*-(3,3,3-trifluoro-1-isopropyl-2-oxopropyl)acetamide (**2e**) (0.67 g, 1.27 mmol) in acetone (10 mL) was combined with dimethyldioxirane generated in acetone (250 mL, 0.028 M, 7 mmol), and the mixture was allowed to stir for 0.5 h. The solvent was evaporated and the residue purified by chromatography, eluting with methanol:dichloromethane (gradient, 10:90 to 20:80), to provide **2h** (0.41 g) in 59% yield: TLC R_f = 0.34, methanol:dichloromethane (10:90); NMR δ 0.81 (d, 3, J = 6.8 Hz), 0.86 (d, 3, J = 6.1 Hz), 2.15–2.30 (m, 1), 4.07 (d, 1, J = 2.7 Hz), 4.34 (s, 2), 4.43 (d, 1, J = 16.3 Hz), 4.57 (d, 1, J = 16.3 Hz), 6.19 (d, 1, J = 7.7 Hz), 7.36–7.48 (m, 7), 8.04 (d, 1, J = 7.7 Hz), 8.22 (d, 2, J = 6.9 Hz); MS m/z = 546 (M + 1).

2-[3-[[(4-Carboxybenzyl)oxycarbonyl]amino]-2-oxo-6-phenyl-1,2-dihydro-1-pyridyl]-*N*-(3,3,3-trifluoro-1-isopropyl-2-oxopropyl)acetamide (2j). To a solution of ester **14j** (0.589 g, 1.0 mmol) in tetrahydrofuran (8 mL) was added a solution of lithium hydroxide monohydrate (0.094 g, 2.24 mmol) in water (2 mL). The biphasic mixture was rapidly stirred for 3 h. The mixture was diluted with water (5 mL) and the pH adjusted to about 3 with 10% aqueous hydrochloric acid to give a white precipitate. This mixture was extracted with ethyl acetate (3 times), and the combined extracts were washed with water, brine, dried, evaporated, and dried under vacuum. The product contained unhydrolyzed ester and was again subjected to the same reaction conditions for 5.5 h. The reaction mixture was worked up as before to give a white solid that was crystallized from hot ethyl acetate/hexane to give acid **2j** as a white solid: TLC R_f = 0.41, dichloromethane:methanol:acetic acid (95.5:4:0.5); NMR δ 0.836 (d, 3, J = 6.9 Hz), 0.90 (d, 3, J = 6.9 Hz), 2.2–2.40 (m, 1), 4.11 (d, 1, J = 2.7 Hz), 4.57 (q, 2, J = 18 Hz), 5.31 (s, 2), 6.27 (d, 1, J = 7.5 Hz), 7.38–7.53 (m, 7), 7.58 (d, 2, J = 9 Hz), 8.00 (t, 3, J = 9 Hz); MS m/z = 574 (M + 1).

2-[3-[[(2-Carboxyphenyl)acetyl]amino]-2-oxo-6-phenyl-1,2-dihydro-1-pyridyl]-*N*-(3,3,3-trifluoro-1-isopropyl-2-oxopropyl)acetamide (2n). To 2-[3-[[[2-(benzyloxycarbonyl)-phenyl]acetyl]amino]-2-oxo-6-phenyl-1,2-dihydo-1-pyridyl]-*N*-(3,3,3-trifluoro-1-isopropyl-2-oxopropyl)acetamide (**14n**) (0.6 g, 0.93 mmol) in methanol (50 mL) was added 10% (w/w) palladium on carbon (0.2 g), and the mixture was shaken under a hydrogen atmosphere (3.4 bar) for 3 h. The catalyst was filtered and the solvent evaporated to give a solid that was chromatographed, eluting with methanol:dichloromethane (gradient, 2:98 to 10:90), to give **2n** (0.5 g, 0.90 mmol, 97% yield); TLC R_f = 0.25, methanol:dichloromethane (10:90); NMR (DMSO–D_2O) δ 0.79 (d, 3, J = 6.8 Hz), 0.84 (d, 3, J = 6.7 Hz), 2.55 (m, 1), 4.03 (d, 1, J = 3.3 Hz), 4.13 (s, 2), 4.53 (m, 2), 6.19 (d, 1, J = 7.7 Hz), 7.46 (m, 8), 7.90 (d, 1, J = 7.8 Hz), 8.24 (d, 1, J =7.6 Hz); MS m/z = 588 (M + 1).

Synthesis of 2o: Example of Sequence 4 → 5o → 6o → 2o. *N*-[2-[(*tert*-Butyldimethylsilyl)oxy]-3,3,3-trifluoro-1-isopropylpropyl]-2-(2-oxo-6-phenyl-3-[[(4-pyridylmethoxy)carbonyl]amino]-1,2-dihydro-1-pyridyl]acetamide (5o). Method D: Acylation Using Triphosgene and an Alcohol (R″OH) or an Amine (R″NH2) (Scheme 1, Reagents c). To a solution of **4** (1.00 g, 1.95 mmol) in methylene chloride (17 mL) was added triethylamine (1.91 mL, 13.6 mmol). The resultant solution was cooled to 0 °C and was treated with a solution of triphosgene (288 mg, 2.92 mmol) in methylene chloride (3 mL) over 5 min. The addition syringe was washed with 2 mL of methylene chloride that was then added to the reaction mixture. The reaction mixture was stirred at 0 °C for 45 min, at which time 4-pyridylcarbinol (688 mg, 6.3 mmol) was added as a solid. Stirring was continued 1 h at 0 °C and then overnight at room temperature. The mixture was diluted with methylene chloride, washed (saturated sodium bicarbonate solution), dried, and evaporated to a brown foam. Purification by flash chromatography, eluting with methylene chloride:methanol (50:1), gave **5o** as a yellow-brown solid (1.18 g, 93% yield): TLC R_f = 0.36, eluted twice with dichloromethane:methanol (50:1); NMR (DMSO–TFAd) δ 0.119 (d, 6, J = 5.1 Hz), 0.769–1.0 (m, 15), 1.70–1.84 (m, 1), 3.86 (t, 1, J = 9 Hz), 4.28 (d, 1, J = 9 Hz), 4.34–4.53 (m, 1), 4.53–4.77 (m, 1), 5.56 (s, 2), 6.24 (d, 1, J = 6 Hz), 7.34–7.53 (m, 5), 7.67 (d, 1, J = 9 Hz), 7.99 (d, 1, J = 7.5 Hz), 8.26 (d, 2, J = 6.3 Hz), 8.99 (d, 2, J = 6.3 Hz); MS m/z = 647 (M + 1).

2-[2-Oxo-6-phenyl-3-[[(4-pyridylmethoxy)carbonyl]amino]-1,2-dihydro-1-pyridyl]-*N*-(3,3,3-trifluoro-2-hydroxy-1-isopropylpropyl)acetamide (6o). Using a similar method to that described in general procedure a for removal of the TBDMS group, but with purification of the crude product by trituration with ethyl acetate, **5o** was converted into **6o**: TLC R_f = 0.23, chloroform:methanol (20:1); NMR (DMSO–TFAd) δ 0.858 (d, 3, J = 6.6 Hz), 0.924 (d, 3, J = 6.6 Hz), 1.70–1.74 (m, 1), 3.87 (t, 1, J = 6 Hz), 4.11 (q, 1, J = 6 Hz), 4.30–4.67 (m, 2), 5.5 (s, 2), 6.23 (d, 1, J = 7.5 Hz), 7.33–7.5 (m, 9), 7.94 (d, 1, J = 9 Hz), 7.98 (d, 1, J = 9 Hz), 8.25 (d, 1, J = 6 Hz), 8.99 (d, 1, J = 6 Hz); MS m/z = 533 (M + 1).

2-[2-Oxo-6-phenyl-3-[[(4-pyridylmethoxy)carbonyl]amino]-1,2-dihydro-1-pyridyl]-*N*-(3,3,3-trifluoro-1-isopropyl-2-oxopropyl)acetamide (2o). Using a similar method to that described in general oxidation procedure b, but using chloroform:methanol (gradient, 40:1 to 30:1 to 20:1) for elution in the chromatography, **6o** was oxidized to afford **2o** in 23% yield; TLC R_f = 0.29, chloroform:methanol (20:1); NMR δ 0.793 (d, 3, J = 6.81 Hz), 0.856 (d, 3, J = 6.75), 2.13–2.26 (m, 1), 4.0–4.06 (m, 1), 4.52 (AB q, 2, J = 16.2, 26.7 Hz), 5.25 (s, 2), 6.24 (d, 1, J = 7.5 Hz), 7.71 (d, 1), 7.93 (d, 1, J = 7.5 Hz), 8.56 (d, 2, J = 5.7 Hz); MS m/z = 531 (M + 1).

2-(3-Formamido-2-oxo-6-phenyl-1,2-dihydro-1-pyridyl)-*N*-(3,3,3-trifluoro-1-isopropyl-2-oxopropyl)acetamide (2u). Method B: Acylation Using a Carboxylic Acid (Scheme 2, Reagents e). To a suspension of 1-[[3-(dimethylamino)-propyl]propyl]-3-ethylcarbodiimide hydrochloride (207 mg, 1.08 mmol) in dichloromethane (10 mL) was added formic acid (1.1 mL, 29.0 mmol), and the mixture was stirred at ambient temperature for 10 min. To the resultant solution was sequentially added *N*-methylmorpholine (100 μL, 0.91 mmol) and amino ketone **7** (398 mg, 1.0 mmol). The reaction mixture was stirred at ambient temperature overnight, diluted with dichloromethane (15 mL), and sequentially washed with dilute hydrochloric acid (1 N, 10 mL), saturated sodium bicarbonate (10 mL), and water (10 mL). At this point the product started to crystallize out of the dichloromethane so methanol (~1 mL) was added, resulting in a clear solution. This solution was dried over magnesium sulfate, filtered, and evaporated to yield an orange, oily solid. The crude material was recrystallized from ethyl acetate:hexane (~12 mL:~2.5 mL) to afford **2u** as a white solid that weighed 247 mg (58% yield) after drying in vacuo overnight: TLC R_f = 0.55 (dichloromethane:methanol, 9:1); NMR δ 0.85 (d, 3, J = 6.7 Hz), 0.90 (d, 3, J = 6.7 Hz), 2.1–2.25 (m, 1), 4.4–4.6 (dd, 2), 4.64 (m, 1, exchanges), 8.21 (d, 1, J = 7.75 Hz), 7.3–7.6 (m, 5H), 8.31 (d, 1, J = 7.75 Hz), 8.37 (s, 1), 8.76 (d, 1, J = 6.5 Hz, exchanges), 9.93 (s, 1, exchanges); MS m/z = 424 (M + 1).

2-(2-Oxo-6-phenyl-3-ureido-1,2-dihydro-1-pyridyl)-*N*-(3,3,3-trifluoro-1-isopropyl-2-oxopropyl)acetamide (2v). To a solution of 2-(3-amino-2-oxo-6-phenyl-1,2-dihydro-1-pyridyl)-*N*-(3,3,3-trifluoro-1-isopropyl-2-oxopropyl)acetamide (**7**) (0.30 g, 0.76 mmol) in tetrahydrofuran (5 mL), cooled to 0 °C, was added, dropwise, chlorosulfonyl isocyanate (0.12 g, 0.83 mmol). The reaction mixture was stirred for 10 min, neutralized with saturated aqueous sodium bicarbonate solution (1 mL), and diluted with ethyl acetate (10 mL), and the organic phase was washed with water and brine, dried, and evaporated. Purification by chromatography, using an eluant of methylene chloride:methanol (30:1), followed by overnight vacuum drying (50 °C at 27 Pa), yielded **2v** as a white solid (0.23 g) in 69% yield: mp 227–230 °C dec; TLC R_f = 0.16, dichloromethane:methanol (20:1); NMR δ 0.88 (2d, 6), 2.15 (m, 1), 4.50 (q, 2), 4.65 (d, 1), 6.18 (d, 1), 6.40 (broad s, 2), 7.40 (m, 5), 8.08 (d, 1), 8.35 (s, 1), 8.75 (d, 1); IR (KBr, cm^{-1}) 3470 (broad), 3360, 1760, 1700; MS m/z = 439 (M + 1).

2-(3-Amino-2-oxo-6-phenyl-1,2-dihydro-1-pyridyl)-*N*-(3,3,3-trifluoro-1-isopropyl-2-oxopropyl)acetamide (7).

General Procedure d: Removal of the CBZ Protecting Group in TFMKs Using Hydrogenolysis (Scheme 2, Reagents a). To a solution of **2a** (22.2 g) in ethanol (500 mL) was added 10% (w/w) palladium on carbon (5.55 g). The mixture was shaken under a hydrogen atmosphere overnight. Catalyst was removed by filtration through diatomaceous earth. The filter pad was washed successively with ethanol and methanol. Concentration of the filtrate gave the crude product as an off-white solid (17.2 g). This material was combined with 0.61 g of product generated from a separate run, dissolved in a minimum volume of methanol, diethyl ether was added, and the mixture was allowed to stand overnight. The precipitate was collected and washed with ether to give **7** as an off-white solid (13.9 g).

Alternatively, **General Procedure e: Removal of the CBZ Protecting Group in TFMKs Using Trifluoromethanesulfonic Acid (Scheme 2, Reagents a).** To a solution of 2-[3-[(benzyloxycarbonyl)amino]-2-oxo-6-phenyl-1,2-dihydro-1-pyridyl]-*N*-(3,3,3-trifluoro-1-isopropyl-2-oxopropyl)-acetamide (**2a**) (10 g) and anisole (6.6 g) in dichloromethane (100 mL) at 0 °C was added trifluoromethanesulfonic acid (9 mL, 15.3 g) while maintaining the temperature below 2 °C. The reaction mixture was allowed to warm to room temperature in 30 min and kept at room temperature for a further 45 min before saturated aqueous sodium bicarbonate was added slowly to pH 7. Ethyl acetate was added, the phases were separated, and the aqueous phase was extracted further with ethyl acetate. The combined organic extract was washed with brine, dried, and evaporated. The crude product was purified by trituration with hexane followed by trituration with diethyl ether to give 2-(3-amino-2-oxo-6-phenyl-1,2-dihydro-1-pyridyl)-*N*-(3,3,3-trifluoro-1-isopropyl-2-oxopropyl) acetamide (**7**) (that can be recrystallized from dichloromethane/hexane) as a white solid (4.85 g): TLC R_f = 0.40, ethyl acetate; NMR δ 0.78–0.91 (m, 6), 2.07–2.30 (m, 1), 4.39 (d, 1), 4.49 (d, 1), 4.61 (t, 1), 5.17 (s, 1), 5.98 (d, 1), 6.51 (d, 1), 7.28–7.41 (m, 5), 8.68 (d, 1); MS m/z = 396 (M + 1).

2-[3-(Ethylamino)-2-oxo-6-phenyl-1,2-dihydro-1-pyridyl]-*N*-(3,3,3-trifluoro-1-isopropyl-2-oxopropyl)acetamide (10). To a solution of **7** (0.305 g, 0.771 mmol) and 2,6-lutidine (0.1 mL, 0.848 mmol) in dimethylformamide (4.5 mL) was added ethyl iodide (0.09 mL, 1.16 mmol). After 20 h, further charges of 2,6-lutidine (0.1 mL, 0.848 mmol) and ethyl iodide (0.09 mL, 1.16 mmol) were made. After 5 h, the reaction mixture was added to ethyl acetate and water, and the organic phase was separated, washed with brine, dried, and evaporated. Chromatography, eluting with dichloromethane:methanol (gradient, 99.5:0.5 to 99:1), gave **10** (68 mg) as a yellow solid in 31% yield: TLC R_f = 0.42, dichloromethane:methanol (98:2); NMR δ 0.88 (dd, 6), 1.77 (t, 3), 2.15 (m, 1), 3.09 (m, 2), 4.45 (m, 2), 4.61 (t, 1), 5.37 (brs, 1), 6.07 (d, 1), 6.27 (d, 1), 7.34 (m, 5), 8.70 (d, 1); MS m/z = 424 (M + 1).

Molecular Modeling. Molecular dynamics (MD) simulations were performed using the program AMBER 3.0a[25] and the united atom model. The starting geometry for the enzyme was taken from the X-ray molecular structure of HLE with the third domain of turkey ovomucoid inhibitor (TOMI).[26,27] The noncovalently bound TOMI fragment was removed from the active site and the HLE-bound sugars, which are remote from the active site region, were removed from the structure for computational simplicity. Inhibitors were covalently attached to the hydroxyl oxygen of Ser-195 at the trifluoromethyl ketone carbonyl carbon and were modeled as the oxyanion. The inhibitors (**2a**, **13k**) were aligned in a manner analogous to the observed arrangement for peptidic inhibitors of PPE.[28] The selection of this binding motif has been further supported by the X-ray crystallographic analysis of similar inhibitors in PPE reported in this and following papers. Atomic charges were obtained for the pyridone fragments of the inhibitors via electrostatic potential energy surface (EPS) fit to 6-31G*//6-31G* *ab initio* wave functions calculated with either the program SPARTAN 2.1[29] or Gaussian 88[30] and a modified version of CHELP.[31] EPS derived 6-31G*//6-31G* charges were also employed for the trifluoromethyl, oxyanion portion of the inhibitor. United atom AMBER 3.0a charges for valine were used for the P_1 portion of the inhibitor. All atomic charges for the inhibitors investigated in this work are reported in the supplementary material.

A 20 Å cap of TIP3P water with a weak restoring force[25] was placed over the active site of the enzyme–inhibitor complex. This resulted in the addition of approximately 450 water molecules to the computations. Previous comparisons of trajectories obtained for HLE bound inhibitors under aqueous periodic boundary conditions[32] suggest that the described water cap conditions are a reasonable approximation for the active site region of this enzyme.

Initial structures were minimized for 250 cycles of steepest decent optimization prior to beginning MD. MD was initiated at 10 K and equilibrated to 298 K using an 8.0 Å cut off radius. A time step of 0.001 ps was employed throughout the simulation and data was collected every 0.1 ps. A pair list update was performed every 0.02 ps. Simulations for each enzyme–inhibitor complex were performed over 50 ps, using the final 40 ps for analysis.

In vacuo, molecular mechanics computations were performed using the AESOP force field[8] and the in-house molecular graphics progam ENIGMA.[7] Only those residues within 12 Å of the active site region of the HNE–TOMI X-ray crystal structure were included in these computations.[1b] HLE atoms were constrained to their position in the X-ray structure for these computations. Geometry optimizations using this model refer to optimizations of the inhibitor relative to this portion of the HLE crystal structure.

Pharmacological Testing. (A) In Vitro. The in vitro assay has been previously described in detail.[17] Like the peptide-based TFMK inhibitors of HLE, these TFMKs exhibited slow-binding[33] kinetics and the K_i values reported are the equilibrium values. **(B) In Vivo (AHA).** The acute hemorrhagic assay is a minor modificiation of a published procedure[34] that measures protection against lung damage (hemorrhage) induced in anesthetized hamsters by 50 μg intratracheally administered HLE, as determined by spectrophotometrically measuring the amount of hemoglobin present in lung lavage after 4 h. As we achieved benchmark levels of oral potency, we regularly increased the rigorousness of the in vivo assay, first by decreasing the dose of test compound (e.g., 80, 20, 5, 2.5 mg/kg) and second by increasing the time interval between dosing and HLE challenge from 30 to 90 min.

Acknowledgment. We thank Steve Brooks and Karin Kirkland for the results of bioavailability studies on compound **2a**. We gratefully acknowledge G. A. Petsko for inviting us to collect diffraction data in his laboratory at Brandeis University, and D. Harrison and R. L. Rardin for their assistance in setting up the diffraction experiments.

Supplementary Material Available: Detailed protocols for the bioavailability and X-ray crystallography studies; a listing of the atom centered charges employed in the molecular dynamics simulations; and tables (with standard deviations) of (a) final atomic positional parameters, (b) atomic thermal parameters, and (c) bond distances and angles obtained in the X-ray crystallographic analysis of the **13d**–PPE complex (13 pages). Ordering information is provided on any current masthead page.

References

(1) For previous papers in this series, please see: (a) Brown, F. J.; Andisik, D.; Bernstein, P. R.; Bryant, C. B.; Ceccarelli, C. A.; Damewood, J. R.; Earley, R.; Edwards, P. D.; Feeney, S. W.; Gomes, B. C.; Green, R.; Kosmider, B. J.; Krell, R.; Shaw, A.; Steelman, G. B.; Thomas, R. M.; Vacek, E. P.; Veale, C. A.; Warner, P.; Williams, J. C.; Wolanin, D. J.; Woolson, S. A. Design of Orally Active, Non-peptidic Inhibitors of Human Leukocyte Elastase. *J. Med. Chem.* **1994**, *37*, 1259–1261. (b) Warner, P.; Green, R. C.; Gomes, B. C.; Williams, J. C. Nonpeptidic Inhibitors of Human Leukocyte Elastase. 1. The Design and Synthesis of Pyridone-Containing Inhibitors. *J. Med. Chem.*, in press. (c) Damewood, J. R., Jr.; Edwards, P.D.; Feeney, S.; Gomes, B. C.; Steelman, G. B.; Tuthill, P. A.; Warner, P.; Williams, J.C.; Woolson, S. A.; Wolanin, D.; Veale, C. Nonpeptidic Inhibitors of Human Leukocyte Elastase. 2. Design, Synthesis, and In Vitro Activity of a Series of 3-Amino-6-arylpyridin-2-one Trifluoromethyl Ketones. *J. Med. Chem.*, preceding paper in this issue.

(2) Abbreviations: AHA, acute hemorrhagic assay; ALI, acute lung injury; DMAP, (dimethylamino)pyridine; HPCD, (hydroxypropyl)-β-cyclodextrin; HLE, human leukocyte elastase; HOBT, 1-hydroxybenzotriazole; HSA, human serum albumin; NC, not calculated; ND, not determined; NS, not significant; PBS, phosphate buffered saline; PEG, polyethylene glycol 500; PPE, porcine pancreatic elastase; TEA, triethylamine; TFMK, trifluoromethyl ketone; WSCDI, 1-[3-(dimethylamino)propyl]-3-ethylcarbodiimide hydrochloride.
(3) See detailed discussion in ref 1b and references therein.
(4) For two recent reviews see: (a) Edwards, P. D.; Bernstein, P. R. Synthetic Inhibitors of Elastase. *Med. Res. Rev.* **1994**, *14*, 127–194. (b) Bernstein, P. R.; Edwards, P. D.; Williams, J. C. Inhibitors of Human Leukocyte Elastase. In *Progress in Medicinal Chemistry*; Ellis, G. W., Luscombe, D. K., Eds.; Elsevier: Amsterdam, 1994; Vol. 31, pp 59–120.
(5) The 50% PEG/PBS formulation was utilized because of the poor solubility of **2a** in 10% PEG/PBS, our standard pharmacologic dosing vehicle.
(6) Brewster, M. E.; Simpkins, J. W.; Maninder, S. H.; Stern, W. C.; Bodor, N. The Potential Use of Cyclodextrins in Parenteral Formulations. *J. Parenteral Sci. Technol.* **1989**, *43*, 231–240.
(7) ENIGMA is an in-house molecular graphics program, ZENECA Inc., Wilmington, DE 19897.
(8) AESOP is an in-house molecular mechanics program, Brian B. Masek, ZENECA Inc., Wilmington, DE 19897, derived in part from QCPE 514: Nachbar, R.; Mislow, K. BIGSTRN-3: General-Purpose Empirical Force-Field Program. *QCPE Bull.* **1986**, *6*, 96–97. AESOP employs the MM2 force field parameters; see Allinger, N. L. QCPE no. 395, Indiana University, Chemistry Building 204, Bloomington, Indiana 47401.
(9) For reviews of the molecular dynamics method, see: (a) McCammon, J. A.; Harvey, S. C. *Dynamics of Proteins and Nucleic Acids*; Cambridge University Press: New York, 1987. (b) Brooks, C. L., III; Karplus, M.; Pettitt, B. M. *Proteins. A Theoretical Perspective of Dynamics, Structure and Thermodynamics*; John Wiley & Sons: New York, 1988. (c) van Gunsteren, W. F.; Weiner, P. K. *Computer Simulation of Biomolecular Systems. Theoretical and Experimental Applications*; Escom: Leiden, 1989.
(10) This report is a synopsis of the results obtained with several hundred of 3-amino substituents, many of which are described in the following patent applications: (a) Bernstein, P. R.; Shaw, A.; Thomas, R. M.; Warner, P.; Wolanin, D. J. Heterocyclic Amides Having HLE Inhibiting Activity. European Patent Application 509,769 A2, published October, 21, 1992. (b) Bernstein, P. R.; Thomas, R. M.; Warner, P.; Wolanin, D. J. Lactam Dipeptides Having HLE Inhibiting Activity. Int. Publication Number: WO 93/21212, Oct. 28, 1993.
(11) Sheehan, J. C.; Cruickshank, P. A.; Boshart, G. L. A Convenient Synthesis of Water-Soluble Carbodiimides. *J. Org. Chem.* **1961**, *26*, 2525–2528.
(12) (a) Fearon, K.; Spaltenstein, A.; Hopkins, P. B.; Gelb, M. H. Fluoro Ketone Containing Peptides as Inhibitors of Human Renin. *J. Med. Chem.* **1987**, *30*, 1617–1622. (b) Pfitzner, K. E.; Moffatt, J. G. Sulfoxide-Carbodiimide Reactions. I. A Facile Oxidation of Alcohols. *J. Am. Chem. Soc.* **1965**, *87*, 5661–5670.
(13) (a) Bergeson, S. H.; Edwards, P. D.; Krell, R. D.; Shaw, A.; Stein, R. L.; Stein, M. M.; Strimpler, A. M.; Trainor, D. A.; Wildonger, R. A.; Wolanin, D. J. Inhibition of Human Leukocyte Elastase By Peptide Trifluoromethyl Ketones. In *Abstracts of Papers 193rd National Meeting of the American Chemical Society, Denver, Colorado, April 5–10, 1987*; American Chemical Society: Washington, D.C., 1987; abstract number MEDI 0001. (b) Bergeson, S. H.; Edwards, P. D.; Schwartz, J. A.; Shaw, A.; Stein, M. M.; Trainor, D. A.; Wildonger, R. A.; Wolanin, D. J. U.S. Patent 4,910,190, 1990; Chem. Abstr. **1991**, *114*, 123085m.
(14) If triethylamine was utilized as the base, as was usually the case for acylations, formation of bis-sulfonylated products also occurred, presumably due to the much higher acidity of the sulfonyl NH proton (pK_a ~9.0) as compared to the acyl NH proton ($pK_a > 11$).
(15) Murray, R. W.; Jeyaraman, R. Dioxiranes: Synthesis and Reactions of Methyldioxiranes. *J. Org. Chem.* **1985**, *50*, 2847–2853.
(16) Graf, R. Reactions with *N*-Carbonylsulfamoyl Chloride. *Angew. Chem., Int. Ed. Engl.* **1968**, *7*, 172–182.
(17) Williams, J. C.; Falcone, R. C.; Knee, C.; Stein, R. L.; Strimpler, A. M.; Reaves, B.; Giles, R. E.; Krell, R. D. Biological Characterization of ICI 200,880 and ICI 200,355, Novel Inhibitors of Human Neutrophil Elastase. *Am. Rev. Respir. Dis.* **1991**, *144*, 875–883.
(18) Edwards, P. D.; Hesp, B.; Trainor, D. A.; Willard, A. K. Enzymes as Targets for Drug Design. In *Enzyme Chemistry: Impact and Applications*, 2nd ed.; Suckling, C. J., Ed.; Chapman and Hall: London, 1990; pp 207–218.
(19) Denis M. J. Absorption Processes. In *Comprehensive Medicinal Chemistry*; Hansch, C., Sammes, P. G., Taylor, J. B., Eds.; Pergamon: Oxford, 1990; Vol. 5, pp 1–43.
(20) Since the pH of the assay is 7.6, the morpholine group should exist predominantly in the unprotonated form. Also, other substituents which are sterically similar to the morpholino group do not show similar increases in K_i. Thus development of a reasonable explanation for this observation requires additional studies.
(21) PPE was utilized since native HLE has been reported to produce small crystals which are unsuitable for X-ray analysis, and attempts to cocrystallize HLE with small, reversible, inhibitors have been unsuccessful (see discussion in ref 26).
(22) Robertus, J. D; Alden, R. A.; Birktoft, J. J.; Kraut, J.; Powers, J. C.; Wilcox, P.E. An X-Ray Crystallographic Study of the Binding of Peptide Chloromethyl Ketone Inhibitors to Subtilisin BPN'. *Biochemistry* **1972**, *11*, 2439–2449.
(23) Bernstein, P. R.; Bryant, C. B.; Ceccarelli, C. A.; Damewood, J. R.; Earley, R.; Feeney, S. W.; Gomes, B. C.; Kosmider, B. J.; Steelman, G. B.; Thomas, R. M.; Vacek, E. P.; Williams, J. C.; Wolanin, D. J.; Woolson, S. A.; Veale, C. A. Nonpeptidic Inhibitors of Human Leukocyte Elastase. 4. Design and Synthesis of a Series of Orally Active 5-Amino-Pyrimidinones. *J. Med. Chem.*, manuscript submitted.
(24) Still, W. C.; Kahn, M.; Mitra, A. Rapid Chromatographic Technique for Preparative Separations with Moderate Resolution. *J. Org. Chem.* **1978**, *43*, 2923–2925.
(25) Singh, U. C.; Weiner, P.; Caldwell, J. C.; Kollman, P. A. *AMBER 3.0 Revision A.*, University of California, San Francisco, 1989.
(26) Bode, W.; Wei, A.-Z.; Huber, R.; Meyer, E.; Travis, J.; Neumann, S. X-ray crystal structure of the complex of human leukocyte elastase (PMN elastase) and the third domain of the turkey ovomucoid inhibitor. *EMBO J.* **1986**, *5*, 2453–2458.
(27) Molecular dynamics simulations have also been performed for a related enzyme, Porcine Pancreatic Elastase (PPE): For example, see: Geller, M.; Swanson, S. M.; Meyer, E. F., Jr. Dynamic Properties of the First Steps of the Enzymatic Reaction of Porcine Pancreatic Elastase (PPE). 2. Molecular Dynamics Simultations of a Michaelis Complex: PPE and the Hexapeptide Thr-Pro-nVal-Leu-Tyr-Thr. *J. Am. Chem. Soc.* **1990**, *112*, 8925–8931 and references therein.
(28) Takahashi, L. H.; Radhakrishnan, R.; Rosenfield, R. E., Jr.; Meyer, E. F., Jr.; Trainor, D. A.; Stein, M. X-ray Diffraction Analysis of the Inhibition of Porcine Pancreatic Elastase by a Peptidyl Trifluoromethylketone. *J. Mol. Biol.* **1988**, *201*, 423–428.
(29) SPARTAN 2.0, Wavefunction, Inc., 18401 Von Karman, Suite 210, Irvine, CA 92715.
(30) Gaussian 88, Revision C Version (1988), Gaussian, Inc. 4415 Fifth Avenue, Pittsburgh, PA 15213.
(31) Brenneman, C. M.; Wiberg, K. B. Determining Atom-Centered Monopoles from Molecular Electrostatic Potentials. The Need for High Sampling Density in Formamide Conformational Analysis. *J. Comput. Chem.* **1990**, *11*, 361–373. We thank C. M. B. for sharing his modified version of CHELP with us.
(32) Damewood, J. R., Jr. Unpublished results, ZENECA Pharmaceuticals, Wilmington, DE 19897.
(33) Stein, R. L.; Strimpler, A. M. Catalysis by Human Leukocyte Elastase. 9. pH Dependent Change in the Rate-Limiting Step. *J. Am. Chem. Soc.* **1987**, *109*, 6538–6540.
(34) Fletcher, D. S.; Osigna, D. G.; Hand, K. M.; Dellea, P. S.; Ashe, B. M.; Mumford, R. A.; Davies, P.; Hagmann, W.; Finke, P. E.; Doherty, J. B.; Bonney, R. J. A Comparison of α_1-Proteinase Inhibitor Methoxysuccinyl-Ala-Ala-Pro-Val-Chloromethylketone and Specific β-Lactam Inhibitors in an Acute Model of Human Polymorphonuclear Leukocyte Elastase-induced Lung Hemorrhage in the Hamster. *Am. Rev. Respir. Dis.* **1990**, *141*, 672–677.